



The atmospheric corrosion of quaternary bronzes: The action of stagnant rain water

C. Chiavari^{a,*}, E. Bernardi^b, C. Martini^a, F. Passarini^b, F. Ospitali^c, L. Robbiola^d

^a Dipartimento di Scienza dei Metalli, Elettrochimica e Tecniche Chimiche, Università di Bologna, Via Risorgimento 4, It-40136 Bologna, Italy

^b Dipartimento di Chimica Industriale e dei Materiali, Università di Bologna, Via Risorgimento 4, It-40136 Bologna, Italy

^c Dipartimento di Chimica Fisica e Inorganica, Università di Bologna, Via Risorgimento 4, It-40136 Bologna, Italy

^d Université de Toulouse, CNRS, UMR 5608 TRACES, Maison de la Recherche, 5 allées Antonio-Machado, F-31058 TOULOUSE Cedex 9, France

ARTICLE INFO

Article history:

Received 2 February 2010

Accepted 17 May 2010

Available online 24 May 2010

Keywords:

A. Alloy
A. Copper
B. Weight loss
C. Atmospheric corrosion
C. Selective dissolution

ABSTRACT

The corrosion behaviour of a quaternary bronze UNS C83600 exposed to stagnant acid rain was examined through wet–dry tests. During the tests, parallel monitoring was performed to determine the evolution of both the bronze surface and the weathering solution composition. The results show that the kinetics of bronze oxidation is governed by diffusion through a two-layer patina: an inner Sn-rich layer and an external Cu and Pb-rich layer. The corrosion rate of the alloy decreases with time, but the dissolution of individual metals (Cu, Zn and Pb) in the environment increases with different trends, showing progressive patina destabilisation.

© 2010 Elsevier Ltd. All rights reserved.

1. Introduction

Numerous parameters have an influence on the decay of outdoor bronze monuments. A key role is played by the geometry of exposure to the environment and, in particular, to the cyclic rain events. On bronze (or copper) monuments, different patinas are formed as the surfaces are directly exposed to rainfalls or not [1–7]. In the case of direct exposure to rain, the leaching action (run-off) will continuously wash reaction products away and renew the aqueous phase. Conversely, on bronze not exposed to this runoff phenomenon, surfaces are submitted to stagnant humid deposition and subjected to repetitive wetting and drying sequences. These areas can even be exposed to thick water films, like in the case of relatively complex geometries often encountered by outdoor sculptures, in which rain can collect and stagnate [1,6]. Therefore, natural patinas formed on these regions have different structures and compositions [1,4–6]. Numerous data and exhaustive investigations concerned copper, as for example in [2–4], some focused on the corrosion behaviour of binary or ternary Cu–Sn–(Zn or Pb) alloys [8–17] and data regarding the behaviour of quaternary Cu–Sn–Zn–Pb alloys [7,8,14,18,19] are more rare.

Two main approaches for understanding the corrosion phenomena occurring on bronze surfaces exposed to atmospheric conditions have been considered up to now.

The first one reports information on ancient bronzes with natural outdoor exposure. Mainly they are works performed on monu-

ments in the framework of the conservation of cultural heritage [1,5–8]. In this context, a clear comprehension of the mechanism of formation of patinas is necessary to define a proper conservation strategy. Actually, on ancient bronze statues, the application of corrosion inhibitors is not done on the original alloy, but on a corroded surface, which in fact is a cleaned patina [5]. In addition, as the inhibitor effectiveness is directly related to the chemical adsorption on the substrate, the specific reactivities of the patina can directly affect the performance of applied protective compounds [17,20–22].

The second approach largely concerns the studies of bronze alloy coupons with selected compositions exposed either in a natural atmospheric environment [9–11] or in experimentally controlled conditions [9–19]. For this latter case, research has been undertaken with the aim of investigating the relation between the patina evolution of a quaternary bronze typically used for artistic casting (UNS C83600) and different rain exposure (stagnation or runoff). In a previous companion work [18], the leaching action of the rain in run-off conditions was explored and the corresponding patina characterised. The results showed the tendency of the quaternary alloy to noticeably dissolve in the environment with the formation of a thin porous and non-protective patina, significantly enriched in insoluble Sn oxo-compounds.

This work aims to study, in the early stages, the influences of each metal component on the corrosion behaviour of a quaternary bronze exposed to stagnant rain (without runoff impact). In this condition, the surface is periodically subjected to wetting, stagnation and evaporation of wet deposition, with a consequent change in pH [23]. Here, the condition of stagnant deposition is simulated

* Corresponding author. Tel.: +39 0512093462; fax: +39 0512093467.
E-mail address: cristina.chiavari@unibo.it (C. Chiavari).

through a wet–dry test [2,12,16,24], an accelerated test where specimens are periodically dipped in a corrosive solution. Synthetic acid rain has been used as the corrosive solution, formulated on the basis of real rains collected in the urban area of Bologna, Italy [25]. The reproducibility in the laboratory of the corrosive conditions by using synthetic solutions was previously performed on the same quaternary bronze [18]. In this system, the metal surface is cyclically exposed for 20 min to bulk conditions and for the other 40 min of drying, to thin film conditions, where corrosion processes are closer to the ones taking place in atmospheric exposures (wet/dry ratio of 1/2).

In the present work, the evolution of the corrosion process was followed by monitoring both samples (surface and cross-section characterisation using scanning electron microscopy, energy-dispersive spectrometry with Raman spectroscopy, and X-ray diffraction) and the ageing solution (pH evolution and metal oxidation, using atomic absorption spectrometry). The periodic analyses of the metals dissolved in the solution, as well as the metals remaining in the patina as corrosion products, allow the behaviour of each metal component to be clarified in the corrosion of the alloy from the early stages.

2. Experimental

2.1. Bronze

The G85 bronze alloy (“85 metal” or UNS C83600) is a quaternary alloy (in wt/wt.%: 88.76 Cu, 4.4 Sn, 3.9 Pb, 2.4 Zn, also containing 0.5 Ni and Fe as trace elements) whose microstructure is described in [18]. It is a sand cast bronze, in which Pb globules from 1 up to about 10 μm in diameter, non-miscible in the Cu-rich matrix, mainly remain in the interdendritic spaces. The alloy was cut into sheets of $\sim 2.5 \times 5 \times 0.5$ cm. Before corrosion tests, the specimen surfaces were polished with abrasive papers of decreasing granulometry (up to 1000 grit), degreased by acetone and finally rinsed with distilled water. For each specimen, the initial weight and surface area were then determined.

2.2. Artificial solution

In order to reproduce the composition of the acid rain as closely as possible, synthetic rain was prepared according to the composition of a mixture of weekly natural rain samples (pH <4.5), collected during the winter months in a monitoring atmospheric station in Bologna [19,25] and influenced by the relatively close proximity of the Mediterranean sea. The synthetic rain was prepared with analytical grade reagents and ultra-pure deionised water (18 M Ω). The composition of the synthetic rain used for the tests is: SO_4^{2-} 1.90 mg L $^{-1}$, Cl^- 1.27 mg L $^{-1}$, NO_3^- 4.64 mg L $^{-1}$, CH_3COO^- 0.23 mg L $^{-1}$, HCOO^- 0.05 mg L $^{-1}$, NH_4^+ 1.06 mg L $^{-1}$, Ca^{2+}

0.34 mg L $^{-1}$, Na^+ 0.53 mg L $^{-1}$, H^+ 0.06 mg L $^{-1}$, with a measured pH of 4.25.

2.3. Weathering method

The condition of rainwater stagnation is simulated through an alternating immersion test during which the bronzes are periodically dipped into the synthetic rain solution. A wet and dry device was designed so as to apply the wetting and drying cycles. It conforms to the main conditions required by the standards UNI 4008-66, UNI EN ISO 11130 and ASTM 44. It consists of six glass jacketed cells interconnected and covered by a Teflon cap. In each cell, only one sample is suspended and connected to a mobile bar by a nylon thread passing through the cap. The vertical movement of each sample is related to the vertical displacement of the bar (max. 4 cm s $^{-1}$). The volume of the synthetic rain solution was 0.3 L per cell and the temperature of the cell solution was maintained constant at 298 K by a propylene glycol based water solution circulating through the jacket and connected to a refrigerated/heating circulator. In each cell, the pH of the weathering solution was regularly monitored with a pH probe. Specific software was used to run the bar automatically and to record the parameters of each test. The duration of one wet and dry corrosion cycle was 1 h, corresponding to 20 min of immersion (wet condition) and 40 min of emersion (dry condition). This wet/dry time ratio (1/2) is close to the ratio between rainy and dry days during the week in winter months in Bologna (on average 2/5) [26]. Considering a time of about 20 min for the samples to get dry, a reasonable Time of Wetness (TOW) of 40 min is assumed to correspond to an hourly cycle. Consequently, 1 year of ageing in this condition can be regarded as ~ 5840 h of TOW, which is roughly three times the annual value found in temperate zones [27].

The reported experiments were replicated at least three times. As described in the work plan of Fig. 1, in short-term experiments, bronze sheets were immersed for periods of 1, 4, 7, 15, 24 and 48 h into the same solution that was not renewed, whereas for long-term ageing, specimens were exposed for 1 up to 8 weeks.

Furthermore, for long-term exposures, two test procedures were applied:

- (i) test solution not renewed (up to 4 weeks);
- (ii) test solution weekly renewed (up to 8 weeks).

A comparison between the first 4 weeks of these two test procedures was carried out in order to investigate the role of pH on the corrosion behaviour in stagnant rainwater conditions. The variation of the pH with time is reported in Fig. 2. The results of tests (i) (solution not renewed) show that, after about 1 week of immersion, the pH value of the stagnant solution stabilizes around 7 and remains neutral up to the fourth week. Conversely, for tests (ii), weekly fresh solution replaced in the cell restores the original

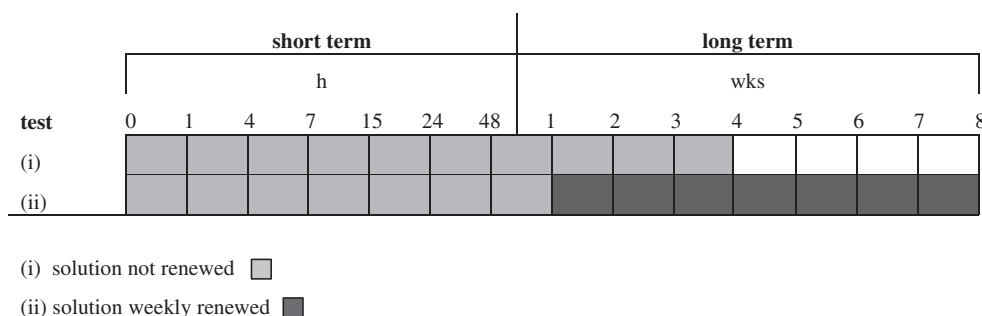


Fig. 1. Work plan of the wet and dry corrosion tests.

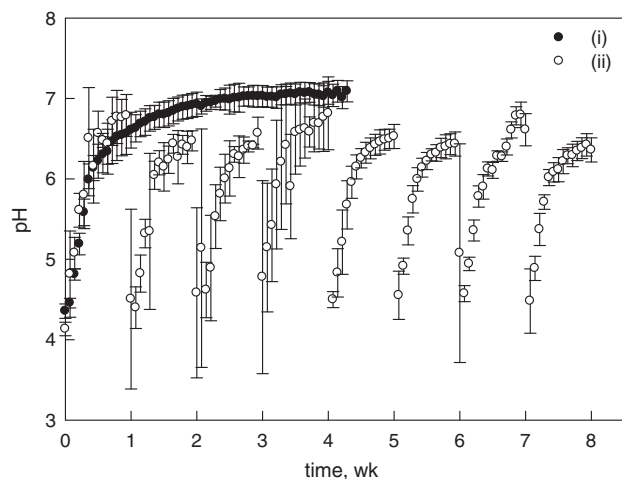


Fig. 2. pH evolution of the ageing solutions in tests (i) and (ii) as a function of exposure time.

acidic pH. According to [23], the test (ii) is a better simulation of the real conditions of exposure of artefacts non-submitted to runoff effects, where the surfaces are cyclically submitted to wetting and evaporation processes with a subsequent change of pH.

To this regard, the important role of pH in the corrosion of unalloyed copper or copper base alloys and in the chemistry of corrosion products is well known [2,7,8,23]. However, in the case of alloys, the way in which each single alloying element reacts towards pH variations is a less investigated topic. This point is of prime importance to better comprehend the mechanism of the destabilisation of bronze patinas known to be linked to acid rains [7,8].

2.4. Solution analyses

At the end of each experiment, weathering solutions were characterised. The concentration of metal cations released in the rain solution, $m_{M,sol}$ with $M = \text{Cu, Sn, Pb or Zn}$, was determined by Atomic Absorption Spectroscopy (AAS; Perkin-Elmer AAnalyst 400). Before the metal analysis, the weathering solutions were collected in HDPE bottles, acidified at $\text{pH} < 2$ with HNO_3 65% suprapur and stored at 4°C . Zn was analysed through Flame AAS, while Cu, Sn and Pb through Graphite Furnace AAS, using pyrolytic graphite tubes with L'vov platform. For the Sn determination, $\text{Mg}(\text{NO}_3)_2$ was added as a matrix modifier ($1 \mu\text{L}$ of $\text{Mg}(\text{NO}_3)_2$ 10,000 mg/L for $20 \mu\text{L}$ of sample). The Limits of Detection (LOD) were: $\text{LOD}_{\text{Cu}} = 0.6 \mu\text{g/L}$; $\text{LOD}_{\text{Sn}} = 1.2 \mu\text{g/L}$; $\text{LOD}_{\text{Pb}} = 0.6 \mu\text{g/L}$; $\text{LOD}_{\text{Zn}} = 1 \mu\text{g/L}$.

2.5. Bronze surface analyses

The nature and evolution of bronze surfaces were characterised from both surface and cross-section investigations. The morphology of the corrosion products was characterised by Optical Microscopy (OM) and by Scanning Electron Microscopy (SEM) in variable pressure mode (Extended Pressure – SEM), coupled with Energy-Dispersive Spectrometry (EDS) for local elemental analyses (INCA ENERGY 350 system – thin film window detector). The quantification was obtained using system supplied standards applying standard ZAF correction factors. Analyses were performed at 20 kV (emission depth around $1 \mu\text{m}$). As a matter of fact, the EDS measurements on thin corrosion layers also integrate a signal emission from the bulk alloy. In fact, as shown later, according to weight loss measurements and considering the density for the patina, the thickness of bronze patina is no more than $1 \mu\text{m}$ for most exposure periods. This point is taken

into account later in the presentation and discussion of EDS results. The corrosion products were characterised by X-ray Diffraction (XRD) using a powder diffractometer (Bragg–Brentano geometry) with a $\text{Cu K}\alpha$ source ($\lambda = 0.15406 \text{ nm}$). Raman microspectroscopy was also carried out by employing the structural and chemical analyser (Raman SCA – Renishaw), which integrates a Raman microprobe (Ar^+ laser, 514.5 nm) in the SEM. The coupling of SEM, EDS and Raman spectroscopy gives complementary information on morphology, elemental composition and molecular characterisation of compounds, with a spatial resolution in the micrometric range. Further experimental details have already been reported in [18].

In addition, mass variation of bronze before and after each test was also carried out. Mass measurements were achieved by a digital balance KERN AGB210.4 with a repeatability of $\pm 0.1 \text{ mg}$. The total mass of alloy which has been oxidised (m_{tot}) was determined from weight loss measurements performed after removing the corrosion layer through a pickling procedure. Different methods have been tested in order to efficiently pickle the heterogeneous patina. In our previous companion work [18], the standard procedure ASTM G1-03 for copper and copper alloys showed significant problems in removing Sn corrosion products and m_{tot} was determined from the measurement of the corrosion thickness. Here, after testing different combinations of etchants on patina dissolution, the following procedure was evaluated as the most effective: preliminary washing in distilled water (1.8 ml cm^{-2}) for 30 s, immersion in HCl 2.4 M (5.3 ml cm^{-2}) for 1 min, washing in distilled water for 30 s. All steps were carried out in an ultrasonic bath, at room temperature. The sequence was repeated twice. The pickling was also performed on an unexposed surface to check self corrosion effects and the results obtained were used as blank test values. The solutions (both water and acid) used in the pickling procedure were then collected and analysed by AAS in order to determine the amount of each metallic element M remaining in the patina, $m_{M,cor}$ with $M = \text{Cu, Sn, Pb or Zn}$. The mass loss of each alloying element M ($m_{M,tot}$), that is the total amount of M which has been oxidised from its metallic state to metal cation during exposure, was determined as follows:

$$m_{M,tot} = m_{M,sol} + m_{M,cor} \quad (1)$$

It must be noticed that m_{tot} , previously defined from the weight loss of the bronze after pickling, can also be computable from the addition of all values $m_{M,tot}$. In this study, the results obtained from these two methods for determining m_{tot} are in agreement with each other: a maximum deviation of 5% was found.

From the previously defined $m_{M,sol}$, m_{tot} , $m_{M,cor}$ and $m_{M,tot}$ several parameters were calculated as defined hereafter.

2.6. Dissolution factor and corrosion rate

In order to quantify the tendency of each alloying element M to dissolve in the corrosive environment and not to remain in the patina, a dissolution factor f_M is defined by analogy to [5,8,19] as:

$$f_M = \frac{m_{M,sol}}{m_{M,tot}} \quad (2)$$

The dissolution factor f_M will range from 0 to 1, according to the tendency of the metal M, initially present in the alloy, to be fully transformed into corrosion products or totally released in the environment, respectively.

The corrosion rate of the alloy is defined as:

$$v_{cor} = \frac{m_{tot}}{A_{cor}t} (\mu\text{g yr}^{-1} \text{ cm}^{-2}) \quad \text{or} \quad v_{cor} = \frac{m_{tot}}{\rho A_{cor}t} (\mu\text{m yr}^{-1}) \quad (3)$$

where ρ is the density of the quaternary bronze ($\rho = 8.954 \pm 0.193 \text{ g cm}^{-3}$), t the time of exposure (yr) and A_{cor} the corroded surface (cm^2).

For each metal element M of the alloy, the corrosion rate $v_{M,cor}$ corresponds to:

$$v_{M,cor} = \frac{m_{M,tot}}{A_{cor}t} \text{ (}\mu\text{g yr}^{-1} \text{ cm}^{-2}\text{)} \quad (4)$$

3. Results and discussion

The results describe the general corrosion behaviour of the quaternary bronze, detailing also the specific behaviour of each metal component. The evolution of the alloying elements in the patina and in the weathering solution is presented for shorter (<48 h) and longer periods (up to 8 weeks). In the latter case, as already highlighted, the comparison between tests (i) and (ii) made it possible to study the influence of pH on the behaviour of the quaternary bronze. The dissolution factors and, finally, the corrosion rates of bronze and of each metallic constituent are reported and discussed.

3.1. Evolution of the corroded bronze surface

Elemental EDS analyses carried out on the bronze surface at different ageing times are reported in Table 1, while the structural characterisations obtained by Raman spectroscopy and XRD analyses are given in Table 2. From these results, the formation of a corrosion layer (patina) is clearly shown right from the first few hours.

It is worth noting that at short-term exposure, the bulk contribution is determinant, being the patina very thin. When the exposure time is increased, some changes in composition are observed, the bulk contributions being lower but always present, as shown by extrapolations of patina thickness versus time. In fact, hypothesizing that patina mainly consists of cuprite ($\rho = 6.0 \text{ g/cm}^3$) and hydrocerussite ($\rho = 6.8 \text{ g/cm}^3$), as discussed below, an average density of 6.1 g/cm^3 was estimated for the patina obtained in test (ii). In these conditions, the thickness (μm) of the patina increases as follows: 0.4 (1 week), 0.6 (2 weeks), 0.8 (4 weeks), 0.8 (7 weeks). Therefore, as the patina thickness is lower than $1 \mu\text{m}$ for all exposure periods, the bulk alloy composition always influences the values measured by EDS on the aged surfaces (see Section 2.5). For this reason, EDS data in Table 1 is also expressed as relative proportions of elements on the surface (element M to copper ratio $(M/Cu)_{cor}$, normalised by the relative proportion in the alloy $(M/Cu)_{alloy}$). Thus, even if the bulk contribution affects the EDS results for longer test periods, some significant changes in composition are observed.

Cu content shows, in the long term, an apparent slight decrease of concentration in the patina, due to the progressive incorporation of the environmental elements, like oxygen, whose content markedly increases after 24 h, and, in lower amounts, chlorine, forming corrosion products identified by Raman and XRD analyses (Table 2). Actually, cuprous oxide is the main constituent of the patina during the whole test. Conversely, copper chlorides are detected after

Table 1
Weight percent of the elements detected on the central area of the aged surfaces at different ageing time, through EDS analyses.

| Test | t | Weight (%) | | | | | | | | | | | |
|-----------|---------|------------|-----|-----|-----|-----|-----|-----|------|------|---------------------------------|---------------------------------|---------------------------------|
| | | Cu | Sn | Pb | Zn | C | O | Ni | Cl | S | $(Sn/Cu)_{cor}/(Sn/Cu)_{alloy}$ | $(Zn/Cu)_{cor}/(Pb/Cu)_{alloy}$ | $(Pb/Cu)_{cor}/(Zn/Cu)_{alloy}$ |
| (i), (ii) | 0 h | 88.7 | 4.4 | 3.9 | 2.4 | | | 0.5 | | | 1 | 1 | 1 |
| (i), (ii) | 1 h | 82.5 | 4.6 | 2.5 | 2.8 | 4.9 | 1.8 | 0.9 | | | 1.12 | 0.69 | 1.25 |
| (i), (ii) | 4 h | 81.2 | 4.6 | 3.6 | 2.7 | 4.3 | 2.7 | 0.8 | | | 1.14 | 1.01 | 1.23 |
| (i), (ii) | 7 h | 78.3 | 4.2 | 5.8 | 2.5 | 4.7 | 3.8 | 0.8 | | | 1.08 | 1.68 | 1.18 |
| (i), (ii) | 15 h | 85.8 | 4.8 | 0.5 | 3.3 | 3.5 | 1.2 | 0.9 | | | 1.13 | 0.13 | 1.42 |
| (i), (ii) | 24 h | 86.2 | 5.0 | 1.1 | 2.9 | 2.8 | 1.1 | 0.9 | | | 1.17 | 0.29 | 1.24 |
| (i), (ii) | 48 h | 77.8 | 4.6 | 1.4 | 1.9 | 2.9 | 10 | 0.7 | 0.26 | | 1.19 | 0.41 | 0.90 |
| (i), (ii) | 1 week | 73.2 | 3.8 | 9.5 | 1.5 | | 11 | 0.5 | 0.35 | | 1.05 | 2.95 | 0.76 |
| (i) | 2 weeks | 66.2 | 3.3 | 16 | 1.9 | | 13 | 0.5 | 0.65 | | 1.00 | 5.50 | 1.06 |
| (ii) | 2 weeks | 73.2 | 3.7 | 9.4 | 1.7 | 4.1 | 11 | 0.6 | 0.37 | | 1.02 | 2.92 | 0.86 |
| (i) | 4 weeks | 67.9 | 3.2 | 8.4 | 1.2 | 6.0 | 12 | 0.5 | 0.50 | | 0.95 | 2.81 | 0.65 |
| (ii) | 4 weeks | 70.7 | 4.4 | 2.0 | 1.6 | 7.7 | 13 | 0.6 | 0.48 | | 1.25 | 0.64 | 0.84 |
| (ii) | 6 weeks | 75.9 | 3.7 | 1.7 | 0.9 | 3.7 | 13 | | 0.71 | | 0.98 | 0.51 | 0.44 |
| (ii) | 7 weeks | 76.6 | 5.4 | 1.7 | 1.5 | 3.8 | 12 | 0.5 | 0.62 | | 1.42 | 0.50 | 0.72 |
| (ii) | 8 weeks | 70.7 | 5.2 | 1.5 | 1.1 | 6.3 | 14 | 0.5 | 0.82 | 0.12 | 1.48 | 0.48 | 0.58 |

Table 2
Corrosion products detected on the surfaces at different ageing time, through Raman and XRD analyses (compounds identified by XRD are labeled with (*)).

| Test | t | Cuprite Cu ₂ O | Cu chlorides CuCl (n) Cu ₂ Cl(OH) ₃ (at) CuCl ₂ ·2H ₂ O (e) | Massicot PbO | Lead sulphates PbSO ₄ (a) | Cerussite PbCO ₃ | Hydrocerussite Pb ₃ (CO ₃) ₂ (OH) ₂ |
|-----------|---------|------------------------------|------------------------------------------------------------------------------------------------------------------|-----------------|-----------------------------------------|--------------------------------|-------------------------------------------------------------------------------------|
| (i), (ii) | 1 h | | | X | | | X |
| (i), (ii) | 4 h | X | | | X | X | |
| (i), (ii) | 7 h | X | | | X | X | X |
| (i), (ii) | 15 h | X* | | | | | X* |
| (i), (ii) | 24 h | X* | | | X | X | X* |
| (i), (ii) | 48 h | X* | | | X | X | X* |
| (i), (ii) | 1 week | X | | X | X(a) | X | X |
| (i) | 2 weeks | X | X (e) | | X | X | X |
| (ii) | 2 weeks | X* | | | | X | X* |
| (i) | 4 weeks | X* | X (at, n*) | X* | | X | X* |
| (ii) | 4 weeks | X* | | X* | X(a) | X | X* |
| (ii) | 6 weeks | X* | X(n*) | X* | | | X* |
| (ii) | 7 weeks | X* | | X* | | X | X* |
| (ii) | 8 weeks | X | X(e, n*) | X | | | |

(n) = nantokite; (at) = atacamite; (e) = eriochalcite; (a) = anglesite.

longer periods: in test (i), eriochalcite ($\text{CuCl}_2 \cdot 2\text{H}_2\text{O}$) after 2 weeks and the thermodynamically more stable atacamite ($\text{Cu}_2\text{Cl}(\text{OH})_3$) after 4 weeks; in test (ii), nantokite (CuCl) after 6 weeks and eriochalcite after 8 weeks. It must be noted that copper hydroxysulphates, typically found on outdoor bronze statues [1–8], were not detected among corrosion products on artificially aged samples in synthetic rain. On the contrary, Pb sulphates were detected, confirming our previous results that showed the preferential formation of these compounds, thermodynamically more stable than copper sulphates [18,19].

As far as Pb is concerned, the fluctuating trend of concentration shown by EDS analyses (Table 1) is related to the precipitation/dissolution of different species on the surface: Pb(II) oxide (massicot, PbO), carbonates (cerussite, PbCO_3 – hydrocerussite, $\text{Pb}_3(\text{CO}_3)_2(\text{OH})_2$) and sulphates, well crystallized as anglesite (PbSO_4) after 1 week (Table 2). Besides cuprous and lead oxides, lead carbonates are the more abundant and widespread products. This is due to the low solubility product of lead carbonates: in fact, the ionic product between the molar concentration of Pb^{2+} and carbonate ions (calculated considering the solubility of the atmospheric CO_2 in water and the equilibrium of the aqueous CO_2) is always very close to or slightly higher than the solubility products of cerussite (7.40×10^{-14} [29]). This is not the case for other corrosion products present in lower amounts, such as lead sulphates, for which the conditions of formation are only locally reached on the surface.

Concerning Zn, the Zn/Cu ratio decreases by comparison to its relative ratio in the alloy. Zn-based products are not found, accordingly to the known solubility of zinc products in this environment [23].

Finally as shown in Table 1, the Sn concentration on the corroded surface fluctuates around the initial value of the alloy but, conversely to Pb and Zn values normalised to copper, a tendency to increase for longer periods in test (ii) is highlighted. However, in the long term, no Sn compounds are identified on the metal surface by XRD and Raman spectroscopy, conversely to that found in run-off conditions [18]. This apparent contradiction is clarified by EDS analyses performed on cross sections at the end of the test (ii). As shown in Fig. 3, a relative enrichment in Sn with a decrease of Cu concentration is clearly shown in the inner layer of the patina.

Therefore, the stratigraphy of the patina consists of a two-layer structure: an inner layer rich in Sn products, most likely (hydrated) hydroxi-oxides according to previous studies [7–10,18], and an outer layer, mainly consisting of Cu and Pb-containing compounds. The inner Sn-rich layer was not detected by surface analyses due to a combination of factors: the presence of the outer layer, which subsequently hides the inner layer, but also the poor crystallinity of the Sn compounds [7,18], which makes them more difficult to characterise.

In order to determine the absolute values of the alloying metal M contained in the patina $m_{M,cor}$, the pickling solutions were analysed according to the procedure previously described in Sections 2.4 and 2.5. The $m_{M,cor}$ values, reported in Table 3, are not affected by any significant contribution of the metal substrate.

The $m_{M,cor}$ data in Table 3 reveal a slight increase in the Cu content in the patina. Compared to the other alloying elements, a very significant enrichment in Pb-containing products in the patina is also revealed. At 7 weeks for test (ii), the relative proportion of Pb in the patina (Cu 67, Sn 2.3, Pb 29 and Zn 1.1 in wt/wt.%) strongly increases with respect to the initial distribution in the alloy (Table 1). Conversely, the relative proportion of Zn and Sn cations in the patina remains close to the ones in the alloy. It must be noticed that the Cu and Pb enrichments with time was not so evident from Table 1, because EDS data were partly affected by bulk composition. It is thus clearly confirmed that the composition of the patina does not reflect the composition of the alloy in terms of alloying components.

3.2. Kinetics of dissolution of the alloy

As shown in Fig. 4, depicting the evolution of the total mass of alloy oxidised (m_{tot}) with time, the bronze oxidation follows a bilogarithmic law, in good agreement with the usual oxidation process controlled by diffusion of species through a corrosion layer acting as a porous barrier.

In fact, according to Table 4, the corrosion rate v_{cor} of the alloy decreases with exposure time, m_{tot} following the equivalent power law:

$$m_{tot} = At^n \quad (5)$$

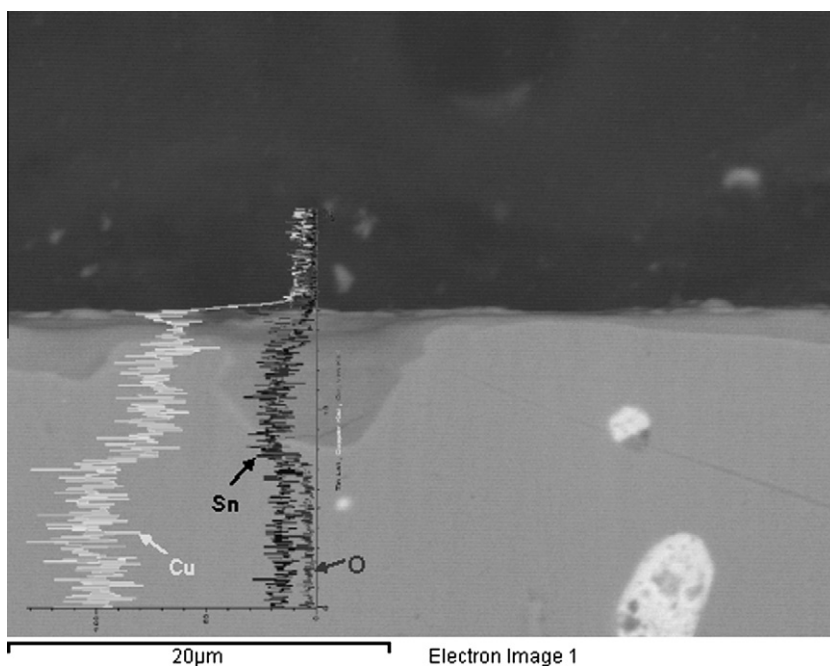


Fig. 3. Cross section of a sample after 8 weeks of exposure by test (ii): BSE image with relative linear EDS map.

Table 3
Evolution of the corrosion parameters ($m_{M,cor}$, $m_{M,sol}$, f_M) with ageing time.

| Test | t | $m_{M,cor}$ ($\mu\text{g cm}^{-2}$) | | | | $m_{M,sol}$ ($\mu\text{g cm}^{-2}$) | | | | f_M | | | |
|-----------|---------|---------------------------------------|---------|-----------|------------|---------------------------------------|---------|--------|--------------------|---------------|-------------|-------------|----|
| | | Cu | Pb | Zn | Sn | Cu | Pb | Zn | Sn | Cu | Pb | Zn | Sn |
| (i), (ii) | 1 week | 162 ± 17 | 96 ± 2 | 0.1 ± 0.1 | 1.4 ± 0.1 | 6 ± 2 | 14 ± 7 | 11 ± 4 | <0.01 ^a | 0.036 ± 0.003 | 0.13 ± 0.06 | 1.0 ± 0.6 | 0 |
| (i) | 2 weeks | n.d. | n.d. | n.d. | n.d. | 11 ± 1 | 26 ± 1 | 8 ± 0 | <0.01 ^a | – | – | – | – |
| (ii) | 2 weeks | 254 ± 20 | 129 ± 3 | 1.6 ± 0.2 | 5.1 ± 0.4 | 25 ± 3 | 40 ± 8 | 14 ± 5 | <0.01 ^a | 0.090 ± 0.006 | 0.24 ± 0.04 | 0.9 ± 0.4 | 0 |
| (i) | 4 weeks | 303 ± 6 | 143 ± 3 | 2.5 ± 0.2 | 9.0 ± 0.1 | 28.4 ± 0.4 | 33 ± 1 | 15 ± 0 | <0.01 ^a | 0.086 ± 0.002 | 0.19 ± 0.01 | 0.86 ± 0.03 | 0 |
| (ii) | 4 weeks | 272 ± 5 | 194 ± 7 | 3.5 ± 0.3 | 6.2 ± 0.3 | 75 ± 4 | 76 ± 10 | 22 ± 5 | <0.01 ^a | 0.217 ± 0.003 | 0.28 ± 0.04 | 0.9 ± 0.2 | 0 |
| (ii) | 6 weeks | n.d. | n.d. | n.d. | n.d. | 138 ± 4 | 92 ± 12 | 29 ± 5 | <0.01 ^a | – | – | – | – |
| (ii) | 7 weeks | 314 ± 10 | 137 ± 2 | 5.1 ± 0.2 | 11.8 ± 0.2 | 172 ± 4 | 96 ± 11 | 33 ± 5 | <0.01 ^a | 0.354 ± 0.008 | 0.41 ± 0.05 | 0.9 ± 0.2 | 0 |
| (ii) | 8 weeks | n.d. | n.d. | n.d. | n.d. | 209 ± 5 | 99 ± 12 | 37 ± 5 | <0.01 ^a | – | – | – | – |

^a Value of Sn for a concentration equal to the limit of detection ($1.2 \mu\text{g L}^{-1}$).

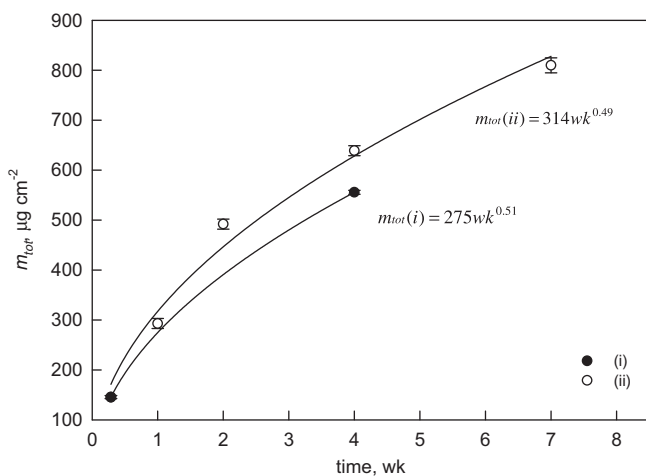


Fig. 4. Mass loss m_{tot} ($\mu\text{g cm}^{-2}$) of the specimens aged by tests (i) and (ii) as a function of exposure time.

(A and n are constant parameters) well agreeing with the typical kinetics controlling the atmospheric corrosion of metals [23]. From Fig. 4, with mass loss expressed in $\mu\text{g cm}^{-2}$ and t in week, for both tests (i) and (ii) the interpolating equation is found to be:

$$m_{tot} \sim 300t^{0.5}. \quad (6)$$

As the n value of the curve fit is close to 0.5, therefore, the rate-controlling step of the corrosion mechanism can be considered the diffusion through a porous layer [23,28].

3.3. The role of the alloying elements

The above described global trend has to be linked to the individual behaviour of the alloying elements. This can be explained through the quantitative analyses of metallic elements dissolved in the weathering solution ($m_{M,sol}$) or remaining in the patina ($m_{M,cor}$) (Figs. 5–7, Tables 3 and 4). On the basis of these results, the decrease of the global corrosion rate v_{cor} previously shown can be mainly ascribed to Cu and Pb corrosion. In fact the corrosion

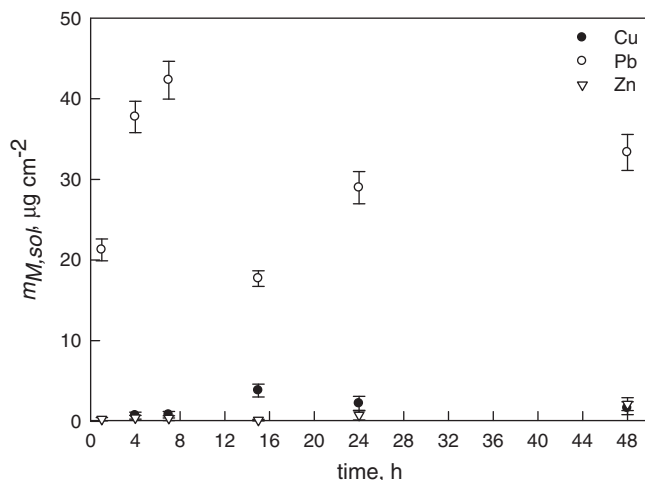


Fig. 5. Metals dissolved in the ageing solution, $m_{M,sol}$ ($\mu\text{g cm}^{-2}$), as a function of exposure time (short-term).

rates of Cu ($v_{Cu,cor}$) and Pb ($v_{Pb,cor}$) decrease during the test, while those of Zn and Sn remain almost constant, but higher for Zn than for Sn (Table 4). Thus, the bronze corrosion is not uniform with respect to the different alloying elements.

During the entire test period and as shown in Fig. 5 and Table 3, at the exception of Sn which is not detected in the solution, the amount of dissolved metal elements in the stagnant solution increases with time. However, and conversely to the behaviour highlighted in run-off condition [18], the concentration of dissolved Cu and Pb ($m_{M,sol}$, Table 3) is significantly lower than that remaining in the patina ($m_{M,cor}$, Table 3), clearly indicating the patina layer built up in stagnant water during the cyclic wetting and drying sequences.

A significant increase is particularly observed for $m_{Cu,sol}$ and $m_{Pb,sol}$ (Fig. 5), but in the short-term Pb dissolution is much more pronounced than Cu dissolution. This particular behaviour of Pb at early stages has to be compared with the evolution of the bronze mass variation depicted in Fig. 6. A clear negative correlation between these two curves is shown. The decrease of mass (mass var-

Table 4

Metal corrosion rate $v_{M,cor}$ ($\text{mg cm}^{-2} \text{yr}^{-1}$) calculated from eq. (4) and adding $m_{M,cor}$ to $m_{M,sol}$, and alloy corrosion rate v_{cor} ($\text{mg cm}^{-2} \text{yr}^{-1}$ and $\mu\text{m yr}^{-1}$) determined from eq. (3) with weight loss m_{tot} determined after pickling, at different ageing times.

| Test | t | $v_{M,cor}$ ($\text{mg cm}^{-2} \text{yr}^{-1}$) | | | | v_{cor} | |
|-----------|---------|----------------------------------------------------|-----------|-------------|---------------|------------------------------------|-----------------------|
| | | Cu | Pb | Zn | Sn | $\text{mg cm}^{-2} \text{yr}^{-1}$ | $\mu\text{m yr}^{-1}$ |
| (i), (ii) | 1 week | 8.8 ± 0.9 | 5.7 ± 0.4 | 0.6 ± 0.2 | 0.074 ± 0.002 | 15.2 ± 0.1 | 17.0 ± 0.4 |
| (ii) | 2 weeks | 7.2 ± 1.0 | 4.4 ± 0.4 | 0.4 ± 0.2 | 0.13 ± 0.02 | 12.8 ± 0.1 | 14.3 ± 0.3 |
| (i) | 4 weeks | 4.0 ± 0.3 | 2.1 ± 0.2 | 0.21 ± 0.02 | 0.11 ± 0.01 | 6.80 ± 0.05 | 7.6 ± 0.2 |
| (ii) | 4 weeks | 4.5 ± 0.2 | 3.5 ± 0.6 | 0.3 ± 0.2 | 0.08 ± 0.02 | 8.31 ± 0.04 | 9.3 ± 0.2 |
| (ii) | 7 weeks | 3.6 ± 0.6 | 1.7 ± 0.6 | 0.3 ± 0.2 | 0.080 ± 0.003 | 6.02 ± 0.03 | 6.7 ± 0.1 |

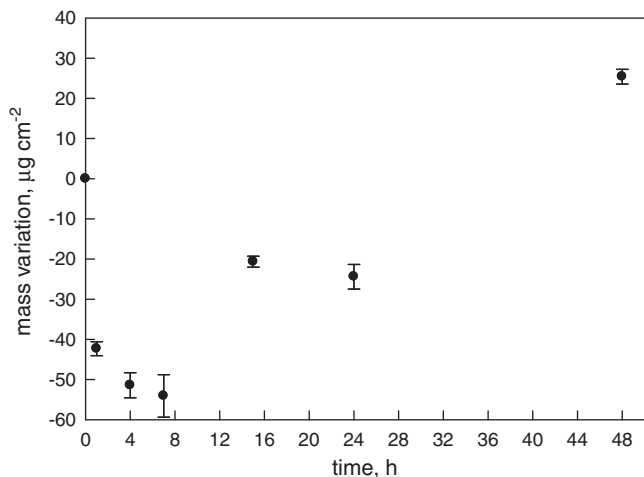


Fig. 6. Mass variation ($\mu\text{g cm}^{-2}$) of the specimens as a function of exposure time: short-term, test (i).

iation vs. time, Fig. 6) in the first stages (up to 7 h) corresponds to an increase of the amount of dissolved Pb ($m_{\text{Pb},\text{sol}}$ in Fig. 5). Similarly, also the remarkable positive variation of the bronze mass from 7 to 15 h corresponds to a strong decrease in the amount of dissolved Pb. Therefore, in the short-term, initial mass variations of bronze are mostly determined by the behaviour of Pb.

Thus, during the first hours, the corrosion of the quaternary bronze is marked by an important oxidation of Pb accompanied by its extensive dissolution. A reason for this can be found in the surface preparation of the specimens, according to [15,18,21]. In

fact, quite analogous to surface finishing performed on artistic castings, this operation would spread the ductile Pb on the surface of the specimen leading to the formation of a thin film of lead oxides. The dissolution of this “artificial” film, a kind of surface etching, is also shown by the initial fast dissolution of Pb occurring up to 15 h (Fig. 5). During this period, the dissolution of the alloy, Cu and Zn metals in particular, is therefore, delayed. The actual dissolution of the bulk alloy starts from about 15 h, but it remains partially hindered by the presence of Pb products.

In the long term (Tables 3 and 4), it is also clearly demonstrated that the corrosion of the alloy is not uniform. In fact, if a general and uniform corrosion of the alloy would take place, at each exposure time, the theoretical amount of oxidised alloying metal M, $m_{M,\text{tot}}^*$, should be related to the total amount of oxidised alloy, m_{tot} , by the following equation:

$$m_{M,\text{tot}} = \chi_M \cdot m_{\text{tot}} \quad (7)$$

where χ_M is the metal weight fraction in the alloy (Table 1) and m_{tot} is reported in Fig. 5. However, the values of $m_{M,\text{tot}}^*$, evaluated by Eq. (7) in the hypothesis of uniform corrosion, do not match the experimental values $m_{M,\text{tot}}$ obtained from Eq. (1), with $m_{M,\text{cor}}$ and $m_{M,\text{sol}}$ given in Table 3. In particular, $m_{\text{Pb},\text{tot}} > m_{\text{Pb},\text{tot}}^*$: this exceeding amount of oxidised Pb clearly indicates a preferential oxidation of Pb, which slows down the oxidation of Zn and Cu. This should be ascribed to the galvanic coupling between different alloy phases. As Pb is immiscible in the (Cu–Sn–Zn) solid solution, the Pb globules in the alloy appear to act as local anodes which are preferentially oxidised.

This phenomenon is also well depicted by the values of the corrosion rates expressed for each metal element $v_{M,\text{cor}}$ (Eq. 4), given in Table 4. The corrosion rate of Pb $v_{\text{Pb},\text{cor}}$ is about half that of Cu,

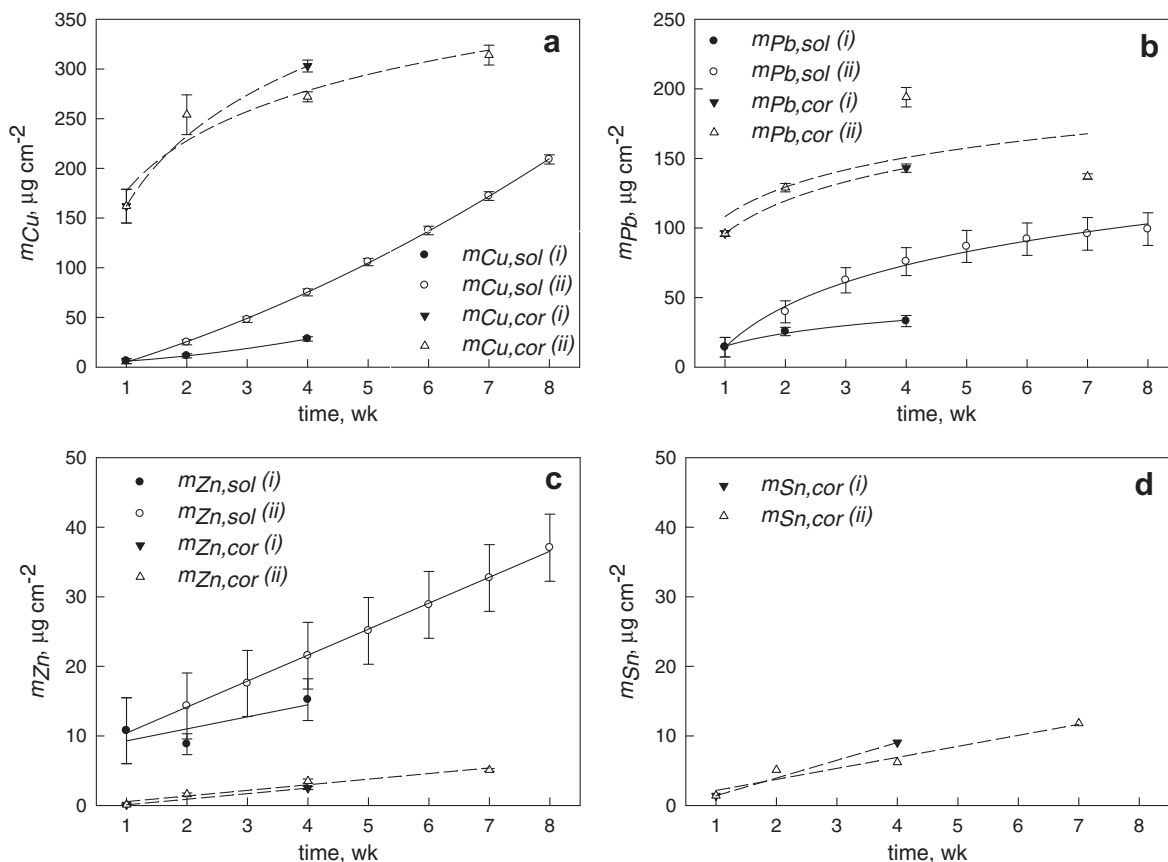


Fig. 7. Metals remained in the patina, $m_{M,\text{cor}}$ ($\mu\text{g cm}^{-2}$), and dissolved in the ageing solution, $m_{M,\text{sol}}$ ($\mu\text{g cm}^{-2}$), during tests (i) and (ii) as a function of exposure time (long term): Cu (a), Pb (b), Zn (c), Sn (d).

while in the alloy the weight ratio Cu/Pb is about 23. This preferential Pb oxidation limits the dezincification, typically observed in ternary alloys (CuSnZn) [10,11,23].

As far as Sn is concerned, Sn content in the patina is systematically lower than expected in the case of a uniform corrosion. Furthermore, it is not detected in the solution. Even hypothesizing a maximum concentration of Sn equal to the detection limit (i.e. $\sim 0.01 \mu\text{g cm}^{-2}$ here), it is clearly shown that the amount of Sn released in the solution is negligible, in good agreement with the results found on bronzes exposed in a natural and artificial urban environment [7–11]. Consequently, it could be assumed that the Sn content is lower than expected in the patina in the case of a uniform corrosion, and null in the solution because forming insoluble oxides. Sn in bronze partly passivates and its corrosion rate $v_{\text{Sn,cor}}$ has the lowest value (Table 4). Therefore, as already pointed out in Fig. 3, the oxidised Sn remains in the inner layer of the patina as insoluble corrosion products according to [9,10,17] and confirming the hypothesis reported in [1,5,7,8]. The localisation of Sn-rich areas close to interdendritic spaces, due to coring phenomena during solidification, makes these oxides non-protective for the whole alloy.

In fact, this inner Sn-rich layer probably behaves like a discontinuous barrier through which Cu, Pb and Zn cations can migrate, precipitate on the surface and/or dissolve in the solution with different trends.

This last point is clearly shown in Table 3 by the different dissolution factors f_M , calculated from the values of $m_{M,cor}$ and $m_{M,sol}$ applying Eq. (2). In stagnant conditions, both in neutralized (test i) and in renewed solutions (test ii), oxidised Cu and Pb tend to remain in the patina ($f_M < 0.5$), even if the amount of metals in solution increases with time. This is particularly true for Cu, where the final value of f_{Cu} is about 10 times higher than at the beginning of the test (Table 3). On the contrary, the high tendency of Zn to fully dissolve in the environment is clearly noticeable from the first week, ($f_{\text{Zn}} \sim 1$). For Sn, the dissolution factor is always zero, because no dissolution was observed. Thus, the dissolution factors globally follow this order: $f_{\text{Cu}} < f_{\text{Pb}} \ll f_{\text{Zn}}$.

A global picture of the corrosion behaviour in stagnant conditions is given in Fig. 7, where the evolution of each metal with time, both in the patina and in the weathering solution for tests (i) and (ii), is summarized.

Three main different behaviours are clearly expressed:

- (a) Cu (Fig. 7a), as well as Pb (Fig. 7b), mainly tend to remain in patina (dashed lines) more than to be dissolved in solution (solid lines). Both exhibit a logarithmic trend for cations remaining in patina, but a different behaviour for dissolved cations. The dissolution of Cu shows a parabolic trend, indicating an acceleration of Cu dissolution in the environment. Conversely, logarithmic kinetics of dissolution are observed for Pb, indicating the tendency to reach a steady state.
- (b) Zn (Fig. 7c) mainly dissolves in solution. In this case, no remarkable difference is observed in the kinetics of oxidation: the amounts of cations both in patina and in the environment show linear increasing trends with low slopes.
- (c) Sn (Fig. 7d) remains only in the patina (inner layer). The oxidation of Sn shows a linear trend, almost not affected by pH of the weathering solution, confirming the formation of insoluble Sn products, non-protective for the alloy, as already observed in binary and ternary bronzes exposed in urban environment [9,10].

3.4. Influence of testing conditions on the corrosion behaviour

The weight of the oxidised alloy m_{tot} remains slightly affected by the periodic variations of both pH and concentration of released cations (Fig. 4, Table 3). The corrosion rates of bronze v_{cor} are sim-

ilar, but slightly lower in the case of not renewed stagnant solution (test i) (Table 4) To this regard, the corrosion rates of each metal element, $v_{M,cor}$, are comparable, except for Pb whose $v_{\text{Pb,cor}}$ is lower in the test (i). This confirms the relevant role of Pb, which mainly conditions the behaviour of the alloy.

Moreover, a higher extent of the dissolution phenomenon is systematically highlighted in test (ii) than in test (i). For example, after 4 weeks, the weight ratio solution/patina for all metal elements is 0.17 in test (i) and 0.36 in test (ii) (Table 3). This confirms that the weekly restoration of the initial acidic solution, significantly increases the dissolution of metallic elements.

As a matter of fact, and as expected, the testing conditions play a major role in the stability of the corrosion compounds of the patina. As Zn mostly dissolves in the environment and Sn totally remains in the patina in both testing conditions, the stability encountered in test (i) has to be related to the higher stability of Pb and Cu compounds of the patina in neutral conditions [23]. Hence, Cu and Pb behaviours are remarkably influenced by the change of solution with a subsequent resetting of the acidic pH, which cyclically destabilises the forming patina. So, it is confirmed that the difference of behaviour here that is obtained after the weekly renewal of the solution (so as to bring the pH back to the original acidic condition) is more related to the destabilisation of the outermost patina rather than to the oxidation process occurring at the inner layer/alloy interface.

In order to compare this value with those obtained in other conditions, such as under runoff exposure, an acceleration factor must be determined. As previously reported in Section 2.3 and 1 year of ageing in this condition corresponds to 5840 h of TOW, which is roughly three times the annual value found in temperate zones [26,27]. Bearing this in mind, the v_{cor} value obtained in this work can be very roughly compared to values found in literature for ternary alloys [10], as well as for bare copper [10,23] resulting in the same order of magnitude. Finally, the corrosion rates here obtained in condition of exposure to stagnant rain water are more than one order of magnitude lower than those of the bronze exposed to severe unsheltered run-off conditions [18].

4. Conclusions

In the present work, the corrosion behaviour of G85 quaternary bronze exposed to stagnant rain was evaluated through an alternating immersion test in artificial acid rain. The parallel analyses on ageing solutions and corroding samples offered an exhaustive picture of alloy dissolution and patina formation, discriminating the behaviour of Cu and other alloying elements. To this regard, the following conclusions can be drawn:

- (1) The kinetics of bronze oxidation is governed by diffusion through a porous layer which forms at initial exposure and grows as time of exposure increases.
- (2) The bronze patina consists of a two-layer structure: an outermost layer, mainly consisting of Cu (oxide and chlorides) and Pb (oxide, sulphates and carbonates) compounds, and an inner layer, enriched in Sn products hardly detectable by surface analyses.
- (3) Sn is not dissolved in the environment and the Sn compounds remain in the inner layer as an insoluble product (likely (hydrated) hydroxi-oxides).
- (4) The global mass variation of the alloy can be related, in the short-term, to an important dissolution of Pb while, in the long term, the evolution of mass loss over time follows a bilogarithmic law.
- (5) By comparison to the relative initial proportion of the metal elements in the alloy, Pb corrodes preferentially. This selective oxidation is probably, in the short-term, in relation with

- a superficial enrichment associated to sample preparation and, in the longer term, in relation with the immiscibility of Pb in the Cu matrix, forming globules which act as sacrificial anodes.
- (6) The amounts of Cu and Pb remaining in the patina are much higher than those dissolved in the stagnant rainwater, conversely to what happens in run-off condition. Zn mostly dissolves in the environment in all conditions (dissolution factor $f_{Zn} \sim 1$).
 - (7) The corrosion rates of the alloy as well as of single metal components decrease with time (except for Sn, for which it remains constant). However, the dissolution of metals in the stagnant solution follows different trends with time: the dissolution of Cu tends to accelerate, the dissolution of Pb tends to reach a steady state, the dissolution rate of Zn is constant. This picture agrees with a progressive destabilisation of the patina with immersion time.
 - (8) The cyclic reconditioning of acidic pH and cations in the solution enhances the phenomenon of destabilisation of the corrosion compounds in the patina, rather the rate of the alloy oxidation.

Acknowledgment

The authors thank Daniele Ciccarella for his contribution to experimental work.

References

- [1] L. Robbiola, L.P. Hurtel, Nouvelle contribution à l'étude des mécanismes de corrosion des bronzes de plein air: caractérisation de l'altération de bronzes de Rodin, *Mémoires et Études Scientifiques Revue de Métallurgie* 12 (1991) 809–823.
- [2] K. Nassau, A.E. Miller, T.E. Graedel, The reaction of simulated rain with copper, copper patina, and some copper compounds, *Corros. Sci.* 27 (7) (1987) 703–719.
- [3] A. Krätschmer, I. Odnevall Wallinder, C. Leygraf, The evolution of outdoor copper patina, *Corros. Sci.* 44 (2002) 425–450.
- [4] K.P. FitzGerald, J. Nairn, G. Skennerton, A. Atrens, Atmospheric corrosion of copper and the colour, structure and composition of natural patinas on copper, *Corros. Sci.* 48 (2006) 2480–2509.
- [5] L. Robbiola, C. Fiaud, S. Pennec, New model of outdoor bronzes corrosion and its implication for conservation, in: *Proceedings of the 10th ICOM Meeting*, vol. II, Washington, 1993, pp. 796–802.
- [6] Dialogue/89, *The Conservation of Bronze Sculpture in the Outdoor Environment: A Dialogue Among Conservators, Curators, Environmental Scientists, and Corrosion Engineers*, Terry Drayman-Weisser Editor, NACE Houston, 1992.
- [7] C. Chiavari, K. Rahmouni, H. Takenouti, S. Joiret, P. Vermaut, L. Robbiola, Composition and electrochemical properties of natural patinas of outdoor bronze monuments, *Electrochim. Acta* 52 (2007) 7760–7769.
- [8] L. Robbiola, K. Rahmouni, C. Chiavari, C. Martini, D. Prandstraller, A. Texier, H. Takenouti, P. Vermaut, New insight into the nature and properties of pale green surfaces of outdoor bronze monuments, *Appl. Phys. A* 92 (2008) 161–169.
- [9] M.T. Sougrati, PhD dissertation – Materials Science, Corrosion Atmosphérique des Bronzes et Spectroscopie Mössbauer, Université de Rouen (France). Available from: <<http://tel.archivesouvertes.fr/tel-00347816/fr/>>.
- [10] S. Jouen, M.T. Sougrati, B. Hannyer, Bronze corrosion and runoff metal dissolution in an urban environment, 17th International Corrosion Congress 2008, Las Vegas, USA, in [9], pp. 214–223.
- [11] G. Herting, S. Goidanich, I. Odnevall Wallinder, C. Leygraf, Corrosion-induced release of Cu and Zn into rainwater from brass, bronze and their pure metals. A 2-year field study, *Environ. Monit. Assess.* 144 (1–3) (2008) 455–461.
- [12] F.J.R. de Oliveira, D.C.B. Lago, L.F. Senna, L.R.M. de Miranda, E. D'Elia, Study of patina formation on bronze specimens, *Mater. Chem. Phys.* 115 (2009) 761–770.
- [13] C. Kleber, M. Schreiner, In situ TM-AFM investigations of the influence of zinc and tin as alloy constituents of copper to the early stages of corrosion, *Appl. Surf. Sci.* 217 (2003) 294–301.
- [14] J.C.D. de Figueiredo, V.D.C. Lins, V.M. De Bellis, Surface characterization of a corroded bronze-leaded alloy in a salt spray cabinet, *Appl. Surf. Sci.* 253 (17) (2007) 7104–7107.
- [15] M. Wadsak, T. Aastrup, I. Odnevall Wallinder, C. Leygraf, M. Schreiner, Multianalytical in situ investigation of the initial atmospheric corrosion of bronze, *Corros. Sci.* 44 (2002) 791–802.
- [16] X. Cao, C. Xu, Synergistic effect of chloride and sulfite ions on the atmospheric corrosion of bronze, *Mater. Corros.* 57 (2006) 400–406.
- [17] F. Ammeloot, C. Fiaud, E.M.M. Sutter, Characterization of the oxide layers on a Cu–13Sn alloy in a NaCl aqueous solution without and with 0.1 M benzotriazole. *Electrochemical and photoelectrochemical contributions*, *Electrochim. Acta* 44 (1999) 2549–2558.
- [18] E. Bernardi, C. Chiavari, B. Lenza, C. Martini, L. Morselli, F. Ospitali, L. Robbiola, The atmospheric corrosion of quaternary bronzes: the leaching action of acid rain, *Corros. Sci.* 51 (2009) 159–170.
- [19] E. Bernardi, C. Chiavari, C. Martini, L. Morselli, The atmospheric corrosion of quaternary bronzes: an evaluation of the dissolution rate of the alloying elements, *Appl. Phys. A* 92 (2008) 83–89.
- [20] G. Brunoro, A. Frignani, A. Colledan, C. Chiavari, Organic films for protection of copper and bronze against acid rain corrosion, *Corros. Sci.* 45 (2003) 2219–2231.
- [21] A. Galtayries, A. Mongiatti, P. Marcus, C. Chiavari, Surface characterisation of corrosion inhibitors on bronzes for artistic casting, in: P. Dillmann, P. Piccardo, H. Matthiesen, G. Beranger (Eds.), *Corrosion of Heritage Artefacts*, Book no. 48, European Federation of Corrosion, 2006, pp. 335–350.
- [22] K. Rahmouni, H. Takenouti, N. Hajjaji, A. Shiri, L. Robbiola, Protection of ancient and historic bronzes by triazole derivatives, *Electrochim. Acta* 54 (22) (2009) 5206–5215.
- [23] T.E. Graedel, C. Leygraf, *Atmospheric Corrosion*, John Wiley and Sons, 2000.
- [24] K.E. García, C.A. Barrero, A.L. Morales, J.M. Greneche, Lost iron and iron converted into rust in steels submitted to dry–wet corrosion process, *Corros. Sci.* 50 (2008) 763–772.
- [25] L. Morselli, E. Bernardi, I. Vassura, F. Passarini, E. Tesini, Chemical composition of wet and dry atmospheric depositions in an urban environment: local, regional and long-range influences, *J. Atmos. Chem.* 59 (2008) 151–170.
- [26] Agenzia Regionale Prevenzione e Ambiente – Regione Emilia Romagna, *Annali Idrologici*, 1998–2008.
- [27] S.E. Manahan, *Fundamentals of Environmental Chemistry*, Lewis Publishers, Chelsea, Massachusetts, 1993.
- [28] P.R. Roberge, *Handbook of Corrosion Engineering*, Technology & Engineering – McGraw Hill Company, 2000 (Chapter 2, p. 86).
- [29] CRC Handbook of Chemistry and Physics, in: D.R. Lide, (Ed.), CRC Press, Taylor & Francis Group LLC, 2008.